Astronomy & Astrophysics manuscript no. mergermetal
February 19, 2010

Metallicity of high stellar mass galaxies with signs of merger events

M. Sol Alonso[1,2], Leo Michel-Dansac[1,3,4], and Diego G. Lambas[1,3]

[1] Consejo Nacional de Investigaciones Científicas y Técnicas, Argentina
e-mail: salonso@icate-conicet.gob.ar, leo@mail.oac.uncor.edu, dgl@mail.oac.uncor.edu
[2] Instituto de Ciencias Astronómicas, de la Tierra y del Espacio, San Juan, Argentina
[3] IATE, CONICET, OAC, Universidad Nacional de Córdoba, Laprida 854, X5000BGR, Córdoba, Argentina
[4] Centre de Recherche Astrophysique de Lyon, Université de Lyon, Université Lyon 1, Observatoire de Lyon, Ecole Normale Supérieure de Lyon, CNRS, UMR 5574, 9 avenue Charles André, Saint-Genis Laval, 69230, France

Received ; accepted

ABSTRACT

Aims. We focus on an analysis of galaxies of high stellar mass and low metallicity. Evidence of recent merger events in their optical images allow us to classify galaxies into either disturbed or undisturbed, and to study galaxy properties such as morphology, colours, stellar populations, and global environment for the different metallicity ranges and disturbance classes.
Methods. We cross-correlated the Millenium Galaxy Catalogue (MGC) and the Sloan Digital Sky Survey (SDSS) galaxy catalogue to provide a sample of MGC objects with high resolution imaging and both spectroscopic and photometric information available in the SDSS database. For each galaxy in our sample, we conducted a systematic morphological analysis by visual inspection of MGC images using their luminosity contours. The galaxies are classified as either *disturbed* or *undisturbed* objects. We divide the sample into three metallicity regions, within wich we compare the properties of disturbed and undisturbed objects.
Results. We find that the fraction of galaxies that are strongly disturbed, indicative of being merger remnants, is higher when lower metallicity objects are considered. The three bins analysed consist of approximatively 15%, 20%, and 50% disturbed galaxies (for high, medium, and low metallicity, respectively). Moreover, the ratio of the disturbed to undisturbed relative distributions of the population age indicator, $D_n(4000)$, in the low metallicity bin, indicates that the disturbed objects have substantially younger stellar populations than their undisturbed counterparts. In addition, we find that an analysis of colour distributions provides similar results, showing that low metallicity galaxies with a disturbed morphology are bluer than those that are undisturbed. The bluer colours and younger populations of the low metallicity, morphologically disturbed objects suggest that they have experienced a recent merger with an associated enhanced star formation rate.

Key words. galaxies: formation - galaxies: evolution - galaxies: abundances - galaxies: interactions.

1. Introduction

In the most commonly accepted cosmological paradigm, galaxy interactions and mergers play a crucial role in determining galaxy properties and are considered as one of the main mechanisms by which galaxies experience significant changes in morphology, stellar population content, and star formation activity (e.g., Barton et al. 2000; Lambas et al. 2003; Alonso et al. 2006). Thus, it is generally accepted that the different merger histories of galaxies define their evolution, origin, and present day properties.

It is also important to consider the chemical properties of galaxies. These can provide fossil records of their history of formation (Freeman & Bland-Hawthorn 2002) since the metallicity content of a galaxy is expected to depend strongly on its evolutionary state, namely, how and when was the gas transformed into stars. The relation between interactions/mergers and chemical properties have been studied by different authors (Donzelli & Pastoriza 2000; Márquez et al. 2002; Fabbiano et al. 2004; Kewley et al. 2006a; Michel-Dansac et al. 2008). The underlying idea in these studies has been that a close companion can induce gas inflows which lower the metallicity in the central regions of galaxies (Kewley et al. 2006a; Michel-Dansac et al. 2008).

A stellar mass-gas metallicity relation has been well established (hereafter MZR, Tremonti et al. 2004). Although it is a clearly observed trend of increasing gas-phase metallicity with stellar mass, there is considerable scatter in the relation, which could be attributed to the particular star formation history of galaxies. Accepted theories for the origin of the MZR have as a central proposition that efficient galactic outflows remove metals from galaxies with shallow potential wells (Larson 1974; Dalcanton 2007; Finlator & Davé 2008). In this context, mergers and interactions could play an important role in determining the shape and scatter of the MZR.

Kewley et al. (2006a) detected a shift in the luminosity - metallicity (LZ) relation towards lower metallicities by ≈ 0.2 dex for galaxy pairs of a given luminosity, compared to a control sample. The spectra analysed in this work corresponded only to the central 10% of the galaxy and the authors interpreted this result as a signature of metal-poor gas being funneled into the center of the galaxies. Following this approach, Ellison et al. (2008) studied the LZ relation of 1716 galaxies with companions with radial velocity $\Delta V < 500$ km.s^{-1} and projected separation rp < 80 kpc h^{-1}, and they found an offset to lower metallicities (by ≈ 0.1 dex) for a given luminosity in pair galaxies. Michel-Dansac et al. (2008) studied the stellar mass - gas metallicity relation of galaxies in close pairs (morphologically classi-

fied according to the strength of the interaction signatures) and in isolation taken from the Sloan Digital Sky Survey Data Release 4 (SDSS-DR4). The authors measured differences in the metallicity of galaxies at a given stellar mass, between pairs showing signs of strong interactions and galaxies in isolation. Thus, the mass-metallicity relation differs between systems with a companion and galaxies in isolation. Interacting galaxy pairs of high stellar mass are found to have systematically lower metallicity values than the mean MZ relation, which implies that gas inflows have been induced by the interaction. In addition, Peeples et al. (2009) studied 42 outliers (massive, metal-poor galaxies) of the MZR in the SDSS, finding that these objects are in general extremely blue and star-forming, and show signs of morphological disturbances.

On larger scales, the MZR appears to be only a weak function of galaxy environment (Mouhcine et al. 2007; Cooper et al. 2008). The gas-phase oxygen abundance of galaxies (at a given stellar mass) in the richest environments is only $\sim$ 0.05 dex higher than those in the poorest environments, and these trends might account for about 15% of the scatter in the MZR. Ellison et al. (2009) explored the impact of cluster membership and local-density on the MZR, confirming that galaxies in clusters are slightly more metal-rich that in the field but that this effect is driven by local overdensity and not simply cluster membership.

Given that the majority of galaxies lie close to the best-fit mass-metallicity relation, we may be able to learn about the gas-phase metallicity evolution of galaxies by studying the properties of galaxies that do not follow this relation. Therefore, joint statistical analysis of mergers/interactions and chemical properties could help us to shed light on the efficiency and extent of the processes mentioned above. To this aim, we consider star-forming, high-stellar-mass galaxies that have in general a well-defined morphology in contrast to smaller systems. It is therefore much easier to identify a recent merger event in these objects. We study high resolution $B-$band images of high mass ($10 < \log M_*/M_\odot < 10.8$) galaxies extracted from the Millennium Galaxy Catalogue (hereafter MGC, Liske et al. 2003; Driver et al. 2005). We classify the galaxies as either disturbed or undisturbed and we explore statistically the effects of recent merger events on oxygen abundance, colour, and stellar age indicators derived from SDSS.

2. Data

Our data consist of galaxies from the Millennium Galaxy Catalogue (Liske et al. 2003; Driver et al. 2005) and the Sloan Digital Sky Server Data Release 4 (Adelman-McCarthy et al. 2006).

The Millennium Galaxy Catalogue is a wide medium-deep $B-$band imaging survey along the celestial equator that was obtained using the Wide Field Camera on the 2.5-m Isaac Newton Telescope on La Palma. The survey covers 37.5 square degrees with $B-$band magnitudes in the range $13 < B < 24$. The survey region coincides with both the 2dF Galaxy Redshift Survey northern strip (2dFGRS, Colless et al. 2001) and the Sloan Digital Sky Survey region (Abazajian et al. 2003).

The SDSS is a photometric and spectroscopic survey that will cover approximately one-quarter of the celestial sphere and collect spectra for more than one million objects. The imaging portion of the fourth release SDSS comprises 6670 square degrees of sky imaged in five wavebands (u, g, r, i, and z) containing photometric parameters of 180 million objects. The spectra

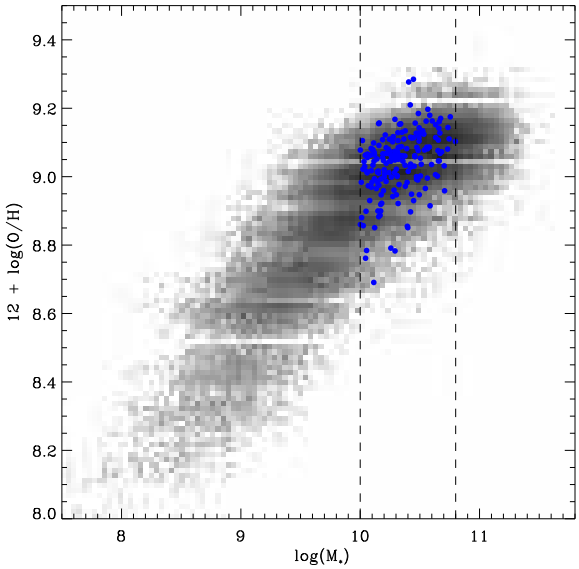

Fig. 1. Stellar mass - gas metallicity relation of a selection of the SDSS galaxies (see text). The vertical dotted lines delimit the mass range that we study in detail in this paper. The blue points correspond to our sample of MGC-SDSS galaxies.

are obtained from 3 arcsec diameter fibers projected on the sky and the coverage is 3800-9200 Å.

The SDSS value-added catalog provides several spectroscopic parameters of physical relevance. However, SDSS imaging is relatively shallow and often taken in poor seeing conditions. Therefore, because we wish to classify galaxies according to their degree of disturbed morphology we use a subset of SDSS galaxies in common with MGC, which provides deeper and higher resolution imaging data. The quality of the images in MGC is a major asset for a detailed study of galaxy morphology. The median seeing of the MGC survey, 1.3 arcseconds (Liske et al. 2003), combined with its deep surface brightness limit of $\mu_B = 26$ mag arcsec^{-2}, provides much higher quality and more clearly resolved images than SDSS images of surface brightness limit 20 mag arcsec^{-2}, which were obtained with a median seeing of 1.5 arcseconds.

We cross-correlated the MGC and SDSS DR4 galaxy catalogs to obtain a sample of MGC objects with oxygen abundances 12 + log(O /H) (Tremonti et al. 2004), stellar mass M_*, and 4000-Å break strength $D_n(4000)$ (Kauffmann et al. 2003), as well as basic information in SDSS data (e.g., redshifts, concentration parameter).

We characterized the local environment of galaxies by defining a projected density parameter, Σ_5. This parameter is calculated by using the projected distance to the 5^{th} nearest neighbour, $\Sigma_5 = 5/(\pi d_5^2)$. Neighbours were chosen to have luminosities brighter than $M_r < -19.5$ and radial velocity differences lower than 1000 km.s^{-1} (Balogh et al. 2004). Kauffmann et al. (2004) estimated the local density by counting galaxies within cylinders of 2 Mpc in projected radius and $\pm$ 500 km.s^{-1} in depth, in a complete sample of galaxies from SDSS. Alonso et al. (2006) found a good correlation signal between both density estimators indicating that either of these two definitions are adequate for characterizing the environment of galaxies. Studies of the relationship between gas-phase oxygen abundance and environment

have used similar parameters, for instance the Σ_3 projected density parameter (Cooper et al. 2008), or a density estimator based on the average of the projected distances to the fourth and fifth nearest neighbour within 1000 km.s^{-1} (Mouhcine et al. 2007).

We imposed an upper redshift cutoff at $z < 0.1$ to ensure both high completeness for both the SDSS and MGC data, and sufficiently high angular resolution. Additionally, we considered a minimum redshift $z > 0.04$ to avoid a too low spatial coverage by the SDSS fibers. Thus, for the range adopted ($0.04 < z < 0.1$) the 3 arcsec SDSS fiber probes approximatively the central 2.5 kpc to 6 kpc of the galaxies.

We restricted the present analysis to high stellar mass objects in the range $10 < \log M_*/M_\odot < 10.8$. The high stellar mass range adopted is consistent with rather extended galaxies so that metallicity measures do not include the external parts of the galaxies. Moreover, the rather narrow stellar mass range adopted ensures that our subsample of galaxies is homogeneous and adequate for the detection of substructures.

To check for any potential AGN contamination in our sample, we analysed the BPT diagnostic diagrams [O III]/Hβ versus (vs.) [N II]/Hα, and both [O III]/Hβ vs. [O I]/Hα and [O III]/Hβ vs. [S II]/Hα proposed by Baldwin et al. (1981), in all cases using the classification criteria given in Kewley et al. (2006b). We found that a small percentage of the objects have line ratios indicative of their spectra being possibly associated with composite AGN/H II regions. To avoid this possibility, we removed these ambiguous cases from the analysis.

A possible concern with SDSS spectroscopy is the signal-to-noise ratio of the relevant lines associated with gas-phase oxygen abundance determinations. We checked that in our sample all galaxies have a signal-to-noise ratio (S/N) of at least 5 in the lines Hα, Hβ, and [N II]λ6584, and at least 3 in the [O III]λ5007 line following the selection criteria of Tremonti et al. (2004). Thus, despite metallicity determination being a complex task with a rather large associated uncertainty, our analysis is not likely to be affected by systematic biases (see also discussion in Sect. 3.2).

With the above restrictions, our final sample comprises 191 high stellar mass galaxies. In Fig. 1, we plot the MZR for the total sample of SDSS galaxies in the redshift range $0.04 < z < 0.1$ satisfying the selection criteria adopted (e.g., AGN removal, S/N), and our sample of high stellar mass MGC-SDSS galaxies. Figure 2 shows the 12 + log(O /H) distribution in both catalogs in 3 mass bins within the mass range selected previously. It can be appreciated that the MZR of our MGC-SDSS sample is truly representative of a MZR determined for the whole SDSS in the selected mass range.

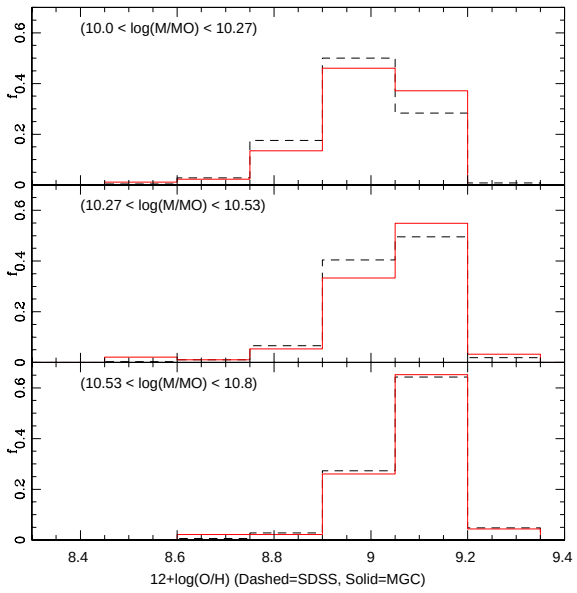

Fig. 2. Oxygen abundance distributions: dashed lines correspond to the SDSS Tremonti et al. data, and solid lines to our sample of MGC-SDSS galaxies in three stellar mass bins.

3. Analysis

3.1. Visual classification of galaxies into disturbed and undisturbed objects

For each galaxy in our sample we conducted a systematic morphological analysis by visual inspecting MGC images and studying the luminosity contours obtained with IRAF routines applied to the reduced images provided in the catalogue. Galaxies are classified as:

a) *Disturbed*: these objects show externally-triggered distortions indicative of a recent strong tidal interaction or merger. Some of these objects exhibit arcs, shells, ripples, tidal debris, warps, rings, extremely asymmetric light distributions, tidal tails, multiple nuclei, and strong substructure inside a common body. We note that these galaxies are not two interacting systems in a ongoing merger, but a single galaxy with signs of being a merger remnant.

b) *Undisturbed*: objects with smooth luminosity contours.

To assess the advantage of using MGC images for the present analysis, we compare in Fig. 3 *B*−band MGC and *g*−band SDSS images for a sample of disturbed galaxies where it is clearly apparent that there is higher reliability when assigning a disturbed morphology in the higher quality MGC data. It is clear that several cases would not be classified as disturbed in SDSS, so that the improvement provided by using MGC data is evident. We also used SDSS data to analyse the close local environment of each galaxy, since MGC images have a too small field of view. Since we are interested in analysing the effects of past merger events, we excluded a few potentially interacting pairs in the sample.

We considered the uncertainty in the visual classification of galaxy morphology by independent determination by different observers. By cross-checking the results, we estimate a 95% coincidence indicating the reliability of our classification scheme.

Visual classification is by nature a subjective task. To assess the reliability of our classification, we derived the asymmetry *A* parameter (Conselice et al. 2000) for the MGC images. Different authors (e.g., De Propris et al. 2007; Jogee et al. 2009) have shown that pairs and galaxy mergers exhibit larger asymmetries. In our sample, for each galaxy, we use SExtractor (Bertin & Arnouts 1996) to calculate the *A* parameter, finding that galaxies classified as *disturbed* by visual inspection have a larger asymmetry parameter ($A \gtrsim 0.30$), and *undisturbed* objects have lower asymmetry values ($A \lesssim 0.30$). More precisely, we find that 72% of disturbed galaxies exhibit $A \gtrsim 0.3$, whereas all the galaxies classified as undisturbed have $A \lesssim 0.3$.

For the stellar mass range explored, we found 46 strongly morphologically disturbed galaxies, 123 undisturbed galaxies, and 22 galaxies with a close companion. The redshift distributions of disturbed and undisturbed galaxies is shown in Fig. 4. The great similarity between these distributions is an indication that our classification is not affected by angular resolution.

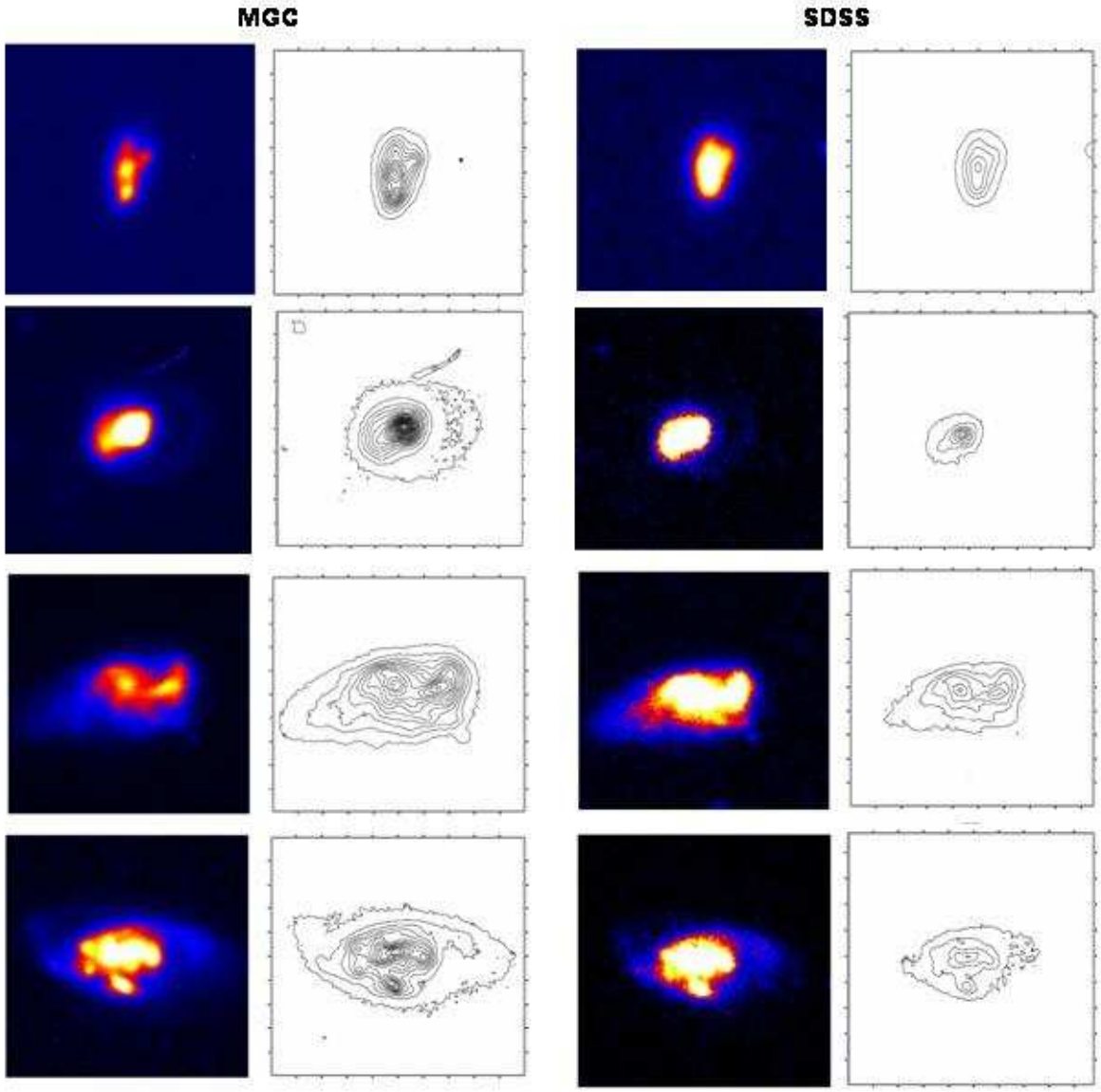

Fig. 3. Images and surface brightness contours of typical massive disturbed galaxies in both MGC (left columns) and SDSS (right columns) catalogs. The image sizes are 33 x 33 arcsec^2.

3.2. Oxygen abundances, colours, and star formation histories of disturbed and undisturbed galaxies

We analysed the oxygen abundance and stellar mass in our sample of high mass MGC-SDSS galaxies. We show the MZR of these galaxies in Fig. 5. We considered two threshold curves displaced with respect to the Tremonti et al. fit, which separate the sample into three regions with low, medium, and high metallicity defined by:

high: $12 + \log(\mathrm{O/H}) > -1.492 + 1.847(\log M_*) - 0.08026(\log M_*)^2 + 0.078$;

low: $12 + \log(\mathrm{O/H}) < -1.492 + 1.847(\log M_*) - 0.08026(\log M_*)^2 - 0.03$;

and a medium metallicity range between these two. Adopted thresholds divide the sample into approximatively 1/4, 2/4, and 1/4 the total sample of galaxies (representing the high, medium, and low metallicity ranges respectively).

As shown in Fig. 5 and Table 1, the relative fractions of disturbed galaxies are statistically significantly different in the three metallicity bins explored. This remarkable tendency for the relative number of disturbed galaxies to increase with decreasing metallicity is also evident from visual inspection of Fig. 5. To quantify these results, we also calculated the percentages of disturbed galaxies for the three different metallicity bins defined previously. At medium and high metallicities, we find that the percentages of disturbed objects are not very different (14% and 21% respectively, cf Table 1). However, at low metallicities, the disturbed galaxy fraction increases remarkably (52%).

To check for possible errors in the metallicities of galaxies in our sample, we recalculated $12 + \log(\mathrm{O/H})$ using the Pettini & Pagel (2004) method, where the oxygen abundance is given by $12 + \log(\mathrm{O/H}) = 9.37 + 2.03 \times \mathrm{N2} + 1.26 \times \mathrm{N2}^2 + 0.32 \times \mathrm{N2}^3$ and $\mathrm{N2} = \log([\mathrm{N\,II}]\lambda6584/\mathrm{H}\,\alpha)$. This method is particularly suited to our sample since all galaxies have a S/N at least 8 in the emission lines used to compute N2. Moreover, the N2 range of the galaxies studied ($-0.7 < \mathrm{N2} < -0.29$) is within the domain of validity for this equation. We considered

Table 1. Number of galaxies classified as disturbed galaxies, undisturbed galaxies, and galaxies with a close companion pairs, in our three ranges of metallicity, and percentages (and respectives sampling errors) of disturbed galaxies with respect to the total number of disturbed and undisturbed galaxies

	disturbed	undisturbed	with close comp.	total	% disturbed
total	46	123	22	191	27.2 ± 3.4
high O/H	6	35	6	47	14.6 ± 5.8
medium O/H	18	68	13	99	20.9 ± 4.4
low O/H	22	20	3	45	52.3 ± 7.7

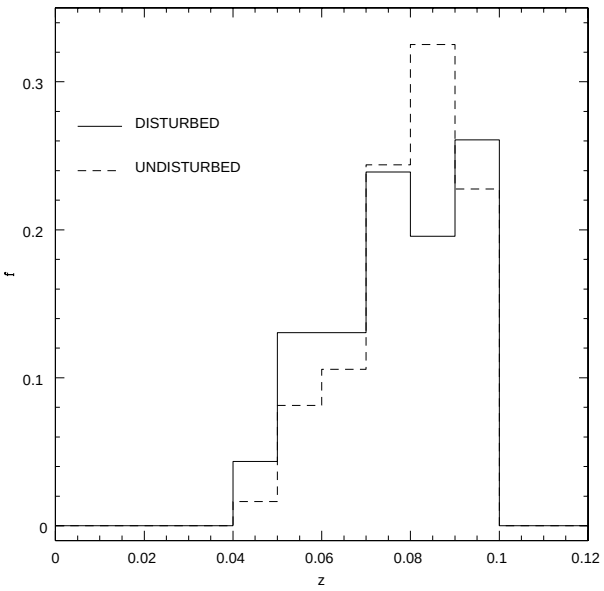

Fig. 4. Redshift distribution of disturbed (solid line) and undisturbed galaxies (dashed line).

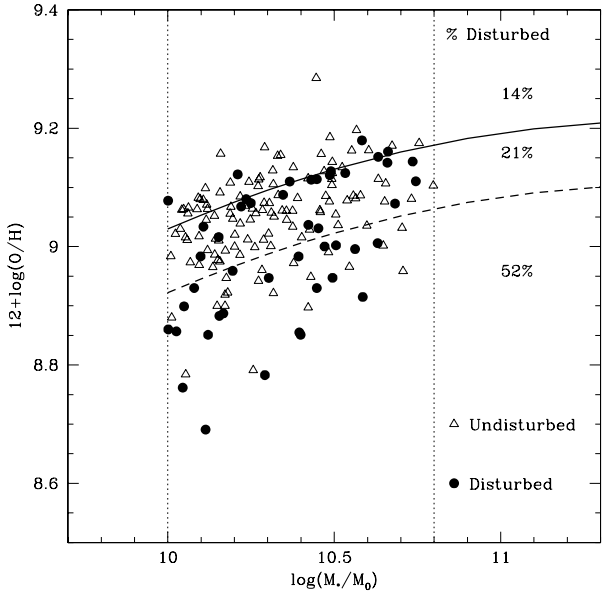

Fig. 5. Distribution of $12 + \log(O/H)$ and $\log(M_*/M_\odot)$ values for galaxies with stellar masses in the range $\log(M_*/M_\odot) \approx 10.0$ to 10.8. The circles correspond to disturbed galaxies and triangles to undisturbed galaxies. The solid and dashed lines indicate the limits of the high, medium, and low metallicity ranges. The solid line corresponds to the Tremonti et al. (2004) fit to the MZ relation shifted by +0.078. The dashed line corresponds to this fit shifted by -0.03 dex.

the three metallicity regions defined previously but shifted by −0.35 dex since this method tends to infer lower values of metallicities than those of Tremonti et al. (2004) (see for instance Kewley & Ellison 2008). With these new estimates, we obtain similar numbers of galaxies in each metallicity bins, as shown in Fig. 6. We also used a subsample of 82 galaxies with data of S/N of at least 8 in the strong emission lines and oxygen abundances measured by Tremonti et al. (2004), finding very similar percentages (63, 22, and 17%) of disturbed galaxies in the low, medium, and high metallicity bins. Then, this trend of increasing the disturbed galaxy fraction at lower metallicity appears robust and is not likely to be caused by errors in the determination of oxygen abundances for these galaxies.

Studies of galaxy properties and their dependence on environment are important for understanding the role of mechanisms driving the evolution of galaxies. We therefore explored the possible influence of the environment of each galaxy in our sample on the results. To this aim, we analysed the local density parameter Σ_5, defined previously, for all galaxies in our sample. The results of this analysis are shown in Fig. 7, where it can be appreciated that disturbed and undisturbed galaxies populate similar environments indicating that the effects are not caused by the particular location of these systems. Thus, we conclude that the strong trend of increasing percentages of disturbed galaxies as a function of decreasing metallicity is not likely to be biased by environmental effects.

For completeness in our analysis, we also studied the light concentration parameter (i.e., the ratio of Petrosian 90% to 50% $r-$band light radii, $C = r_{90}/r_{50}$) of the galaxies in the sample to search for possible differences in our sample between disturbed and undisturbed objects. The concentration index value of $C = 2.5$ was adopted to segregate concentrated, bulge-like ($C > 2.5$) galaxies from more extended, disc-like ($C < 2.5$) systems. In Fig. 7, the similarity between the C parameters across the samples is clearly evident, showing that the observed disturbed to undisturbed ratio dependence on metallicity is probably not associated with systematic differences in the bulge-to-disc ratios of the galaxies. To quantify the significance of the differences between the distributions in Fig. 7, we calculated the occurrence of $C < 2.5$ in galaxies with low metallicities in 20 randomized samples. In each sample, the C parameter was reassigned randomly, in disturbed and undisturbed objects of low metallicity. Since we found that in 6 out of 20 randomized samples the signal is as strong as in the data, we conclude that no statistically significant tendency associated with disturbed and undisturbed galaxies can be identified for the concentration parameter.

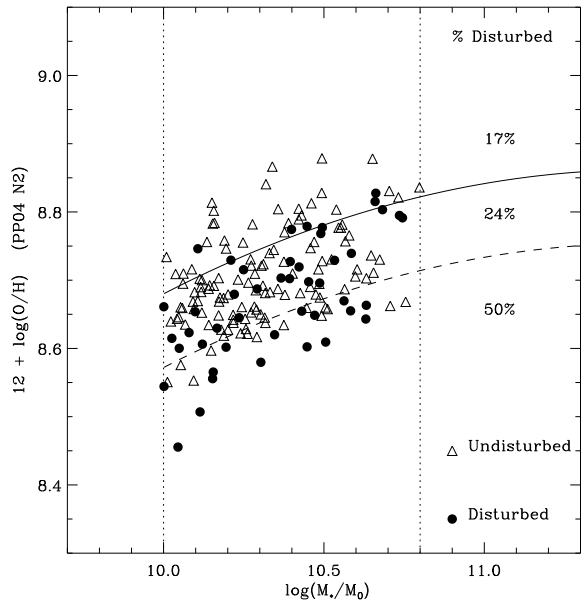

Fig. 6. Distribution of 12 + log(O/H) calculated through the Pettini & Pagel (2004) method, and log($M_*/M_\odot$) values for galaxies with stellar masses in the range log($M_*/M_\odot$) ≈ 10.0 to 10.8. Symbols are the same as in Fig. 5. The solid and dashed lines indicate the limits of the high, medium, and low metallicity ranges. With these abundances, the solid line corresponds to the Tremonti et al. (2004) fit to the MZ relation shifted by −0.272. The dashed line corresponds to this fit shifted by −0.38 dex.

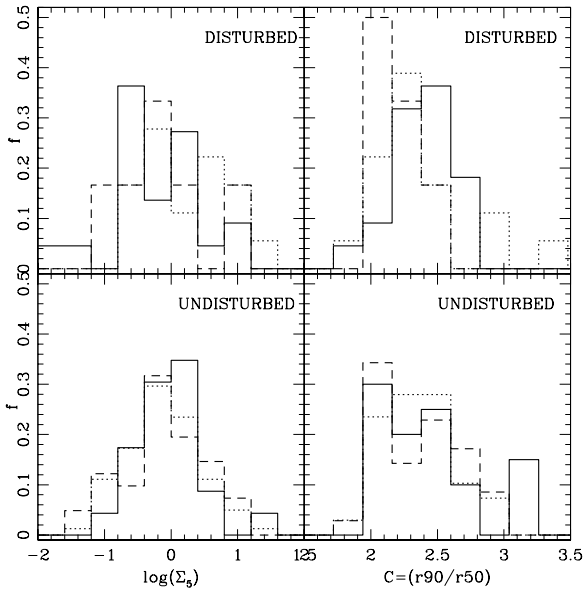

Fig. 7. Distribution of the environmental local galaxy density parameter Σ_5 and image concentration parameter C for disturbed and undisturbed objects in the three metallicity ranges: low (solid), medium (dotted), and high (dashed line).

That the relative fraction of disturbed to undisturbed galaxies increases for low metallicity objects provides important evidence that a merger process induces low metallicity gas inflows. This phenomenon should also be reflected in the mean stellar age population of disturbed objects as a function of metallicity. The $D_n(4000)$ spectral index defined by Bruzual (1983) is a suitable indicator of the current luminosity-weighted mean stellar age since young stellar populations produce almost no metal absorption just shortward of 4000Å. Therefore, galaxies dominated by recent episodes of star formation exhibit a small index, while the spectra of galaxies dominated by older populations exhibit strong metal lines in absorption and thus larger $D_n(4000)$ values. We analysed the $D_n(4000)$ population age indicator in the 3 gas-phase oxygen abundance ranges. The results are shown in Fig. 8, where we plot the fraction of $D_n(4000)$ for disturbed objects normalized to that for undisturbed galaxies (fraction($D_n(4000)(disturbed)/D_n(4000)(undisturbed)$)). We find that at both medium and high metallicity, both disturbed and undisturbed objects have a similar $D_n(4000)$, with a slight tendency for disturbed objects to have older stellar populations. It can also be appreciated that low O/H values objects, where the disturbed population is important, have substantially younger stellar populations than their undisturbed counterparts. Thus, our morphological analysis indicates that in high stellar mass galaxies, low metallicity values are associated with star formation episodes triggered by recent merger events. By adopting the same procedure used previously to quantify the differences between the distributions of the C parameter, we test the differences between the $D_n(4000)$ distributions shown in Fig. 8. Here the results show high confidence in the significance of the differences since none of the 20 randomized realizations exhibit a signal as strong as in the data. We conclude that at low metallicities, disturbed galaxies have a younger stellar population at least at the 95% confidence level.

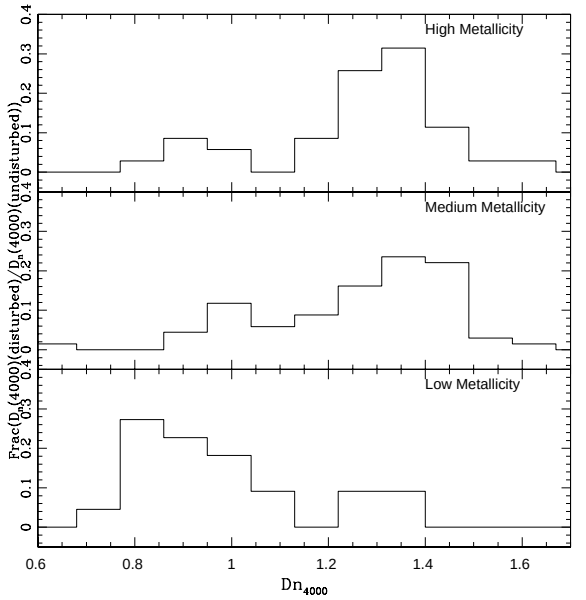

Fig. 8. Fraction of stellar age indicator ($D_n(4000)$) for disturbed normalized to undisturbed galaxies ($D_n(4000)(disturbed)/D_n(4000)(undisturbed)$) in the three metallicity ranges.

We also considered the fraction of disturbed galaxies above the median $D_n(4000)$ for a given value of M_*. By doing so, we aim to relate merging events to the relative fraction of young stellar populations. In Fig. 9, we show the observed $D_n(4000)$ vs M_* for disturbed and undisturbed galaxies. As can be appreciated in this figure (see quoted numbers), there is a larger

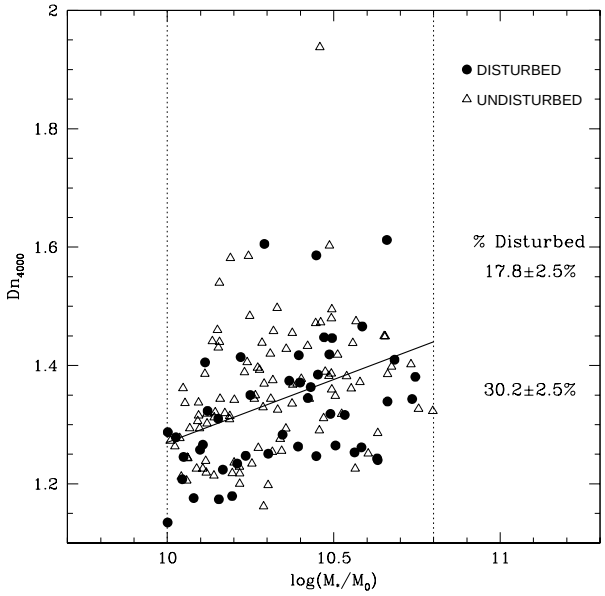

Fig. 9. Distribution of $D_n(4000)$ and $\log(M_*/M_\odot)$ values for galaxies with stellar masses in the range $\log(M_*/M_\odot) \approx 10.0$ to 10.8. The circles correspond to disturbed galaxies and triangles to undisturbed galaxies.

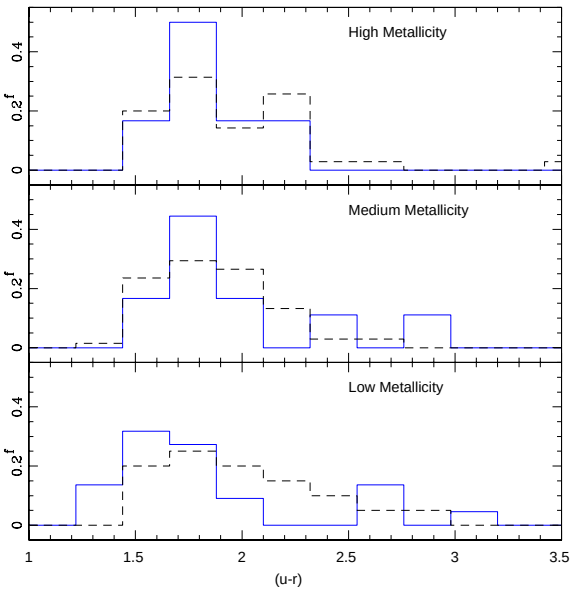

Fig. 10. Colour index $(u-r)$ for disturbed (solid) and undisturbed galaxies (dashed) in the three adopted metallicity ranges.

fraction of disturbed galaxies with stellar population ages above the median defined by $D_n(4000) = 0.2125 \log(M_*/M_\odot) - 0.85$ (shown as a solid line). Thus, our classification of disturbed type selects preferentially galaxies with the highest fraction of young stellar populations at a given stellar mass content, as expected in a merger-induced star formation scenario. We addressed the uncertainties in our estimated fractions of disturbed and undisturbed galaxies by moving the median line threshold of 0.3 dex. We find that the relative fractions do not change significantly indicating that the results are not sensitive to the particular choice adopted.

Observational analyses of the $u-r$ colour distributions (e.g., Alonso et al. 2006; De Propris et al. 2005) have reported an excess of blue colours in close pair galaxies with signs of interactions, relative to those measured for galaxies without close companions. This finding is associated with both a larger fraction of actively star-forming galaxies and younger stellar populations in disturbed close pair systems. In Fig. 10, we compare the $u-r$ colour distributions of disturbed galaxies with those of their undisturbed counterparts. The analysis was performed for the three different metallicity ranges previously considered (see Table 1). We find that in both the high and medium metallicity ranges (upper and medium panels, respectively), the colour distributions of disturbed objects are more similar to those of undisturbed galaxies than in the lower metallicity range. Interestingly, at lower metallicity (lower panel), the colour distributions of disturbed and undisturbed galaxies exhibit significant differences, morphologically disturbed objects having a larger fraction of blue colours. We also observe a significant difference in the blue tail, where there is a clear excess of blue disturbed galaxies with respect to undisturbed objects. The blue excess can be interpreted in terms of substructures associated with externally-triggered distortions, indicative of recent interactions or mergers, and both enhanced star formation and young stellar populations as already shown in Fig. 8.

4. Discussion and Conclusions

Observed metallicity gradients in galaxies (e.g., Zaritsky et al. 1994; Ferguson et al. 1998; Dutil & Roy 1999; Considère et al. 2000) show evidence of less enriched gas in the external regions. Thus, a large low-metallicity gas reservoir is expected in most massive star-forming galaxies. On the other hand, numerical simulations indicate that galaxy interactions and mergers may generate a significant flow of external gas onto the central region and trigger star formation. Thus, interactions may be efficient in lowering the central metal content of galaxies by means of an inflow of this external, less enriched gas.

Similar effects have been reported by Michel-Dansac et al. (2008) and Ellison et al. (2008), where interacting pairs with strong morphological disturbance features have lower metallicities. This is also reinforced by the high mass outliers in the MZ relation exhibiting distorted morphologies (Peeples et al. 2009).

The above considerations have led us to analyse the presence of possible relics of such process in non-interacting, high-stellar-mass galaxies. To this aim, we have performed a morphological analysis of high quality images from the MGC of high-stellar-mass SDSS galaxies. Objects in this mass range have a more clearly defined morphology and so are suitable for exploring morphological disturbances associated with merger events. On the other hand, the oxygen abundance is a clear indicator of the gas phase metallicity and so is sensitive to the presence of recently formed stars.

By construction, our subsamples of high, medium, and low metallicity objects have similar stellar-mass distributions. Moreover, we have confirmed that the subsamples are free of strong biases widely different local galaxy density environments, or widely different concentration parameters so that we expect them to have similar bulge-to-disc ratios. Thus, the subsamples analysed comprise galaxies of similar morphology and environment.

Our main result is that we detect a steadily increasing fraction of morphologically disturbed galaxies, characteristic of being merger remnants, with decreasing O/H. The three bins anal-

ysed consist approximatively of 15%, 20%, and 50% disturbed galaxies (high, medium, and low metallicity, respectively)

Moreover, the ratio of disturbed to undisturbed distributions of the $D_n(4000)$ parameter in both the medium and high metallicity bins are similar, the $D_n(4000)$ values corresponding to a relatively old stellar population in disturbed objects. This contrasts with the results for the low metallicity bin where disturbed objects have a substantially younger stellar populations than their undisturbed counterparts. In addition, the colours distributions exhibit similar trends, showing that low metallicity galaxies with a disturbed morphology are bluer than those that are undisturbed.

The bluer colours and lower $D_n(4000)$ values in low metallicity, morphologically disturbed objects, suggest externally-triggered distortions driven by a recent interaction or merger, with an associated enhanced star-formation rate and a predominance of a young stellar population.

Rupke et al. (2008) showed that ultra-luminous infrared galaxies (ULIRGs) have systematically lower O/H values than star-forming galaxies of similar stellar mass content, consistent with a merger-driven inflow of low metallicity gas. Our results show, in addition, that this mechanism is not only present in ULIRGs but also in high stellar mass galaxies with morphological evidence of a merger event.

The most natural explanation of our results is that merger-induced low metallicity gas inflows have occurred from the external regions of high stellar mass galaxies. Our results also suggest that the timescale of the chemical evolution (the combined effects of the enrichment of the interstellar medium by SNII and these inflows) is at least as long as the timescale of the tidally induced morphological disturbances. Thus, galaxies with a disturbed appearence may contain young stellar populations and yet low gas-phase abundances in their central parts. Our results suggest that, at least in part, the scatter in the MZR at high stellar mass is caused by interactions and mergers.

Acknowledgments

We thank the referee for helpful comments and suggestions. This work was partially supported by the Consejo Nacional de Investigaciones Científicas y Técnicas, the Agencia de Promoción de Ciencia y Tecnología, the Secretaría de Ciencia y Técnica de la Universidad Nacional de Córdoba, and the MinCyT - ECOS-Sud program #A07U01.

The Millennium Galaxy Catalogue consists of imaging data from the Isaac Newton Telescope and spectroscopic data from the Anglo Australian Telescope, the ANU 2.3m, the ESO New Technology Telescope, the Telescopio Nazionale Galileo and the Gemini North Telescope. The survey has been supported through grants from the Particle Physics and Astronomy Research Council (UK) and the Australian Research Council (AUS). The data and data products are publicly available from http://www.eso.org/~jliske/mgc/ or on request from J. Liske or S.P. Driver.

Funding for the SDSS and SDSS-II has been provided by the Alfred P. Sloan Foundation, the Participating Institutions, the National Science Foundation, the U.S. Department of Energy, the National Aeronautics and Space Administration, the Japanese Monbukagakusho, the Max Planck Society, and the Higher Education Funding Council for England. The SDSS Web Site is http://www.sdss.org/.

The SDSS is managed by the Astrophysical Research Consortium for the Participating Institutions. The Participating Institutions are the American Museum of Natural History, Astrophysical Institute Potsdam, University of Basel, University of Cambridge, Case Western Reserve University, University of Chicago, Drexel University, Fermilab, the Institute for Advanced Study, the Japan Participation Group, Johns Hopkins University, the Joint Institute for Nuclear Astrophysics, the Kavli Institute for Particle Astrophysics and Cosmology, the Korean Scientist Group, the Chinese Academy of Sciences (LAMOST), Los Alamos National Laboratory, the Max-Planck-Institute for Astronomy (MPIA), the Max-Planck-Institute for Astrophysics (MPA), New Mexico State University, Ohio State University, University of Pittsburgh, University of Portsmouth, Princeton University, the United States Naval Observatory, and the University of Washington.

References

Abazajian K., et al. 2003, AJ, 126, 2081
Adelman-McCarthy J. K., et al. 2006, ApJS, 162, 38
Alonso M. S., Lambas D. G., Tissera P., Coldwell G., 2006, MNRAS, 367, 1029
Baldwin J. A., Phillips M. M., & Terlevich R. 1981, PASP, 93, 5
Balogh M., Baldry I. K., Nichol R., Miller C., Bower R., Glazebrook K., 2004, ApJ Letters, 615, 101.
Barton E. J., Geller M. J., & Kenyon S. J. 2000, ApJ, 530, 660
Bertin E., & Arnouts S. 1996, A&AS, 117, 393
Brinchmann J., Charlot S., White S. D. M., Tremonti C., Kauffmann G., Heckman T., & Brinkmann J. 2004, MNRAS, 351, 1151
Bruzual A. G. 1983, ApJ, 273, 105
Colless M., et al. 2001, MNRAS, 328, 1039
Considère S., Coziol R., Contini T., & Davoust E. 2000, A&A, 356, 89
Conselice C. J., Bershady M. A., & Jangren A. 2000, ApJ, 529, 886
Cooper M. C., Tremonti C. A., Newman J. A., & Zabludoff A. I. 2008, MNRAS, 390, 245
Dalcanton J. J., 2007, ApJ, 658, 941
De Propris R., Conselice C. J., Liske J., Driver S. P., Patton D. R., Graham A. W., & Allen P. D. 2007, ApJ, 666, 212
De Propris R., Liske J., Driver S. P., Allen P. D., & Cross N. J. G. 2005, AJ, 130, 1516
Donzelli C. J., & Pastoriza M. G. 2000, AJ, 120, 189
Driver S. P., Liske J., Cross N. J. G., De Propris R., & Allen P. D. 2005, MNRAS, 360, 81
Dutil Y., & Roy J.-R. 1999, ApJ, 516, 62
Ellison S. L., Patton D. R., Simard L., & McConnachie A. W. 2008, AJ, 135, 1877
Ellison S. L., Simard L., Cowan N. B., Baldry I. K., Patton D. R., & McConnachie A. W. 2009, MNRAS, 396, 1257
Fabbiano G., et al. 2004, APJL, 605, L21
Ferguson A. M. N., Gallagher J. S., & Wyse R. F. G. 1998, AJ, 116, 673
Finlator K., & Davé R. 2008, MNRAS, 385, 2181
Freeman K., & Bland-Hawthorn J. 2002, ARA&A, 40, 487
Jogee S., et al. 2009, ApJ, 697, 1971
Kauffmann G., et al. 2003, MNRAS, 341, 33
Kauffmann G., et al. 2004, MNRAS, 353, 713
Kewley L. J., & Ellison S. L. 2008, ApJ, 681, 1183
Kewley L. J., Geller M. J., & Barton E. J. 2006a, AJ, 131, 2004
Kewley L. J., Groves B., Kauffmann G., & Heckman T. 2006b, MNRAS, 372, 961
Lambas D. G., Tissera P. B., Alonso M. S., & Coldwell G. 2003, MNRAS, 346, 1189
Larson R. B., 1974, MNRAS, 166, 585
Liske J., Lemon D. J., Driver S. P., Cross N. J. G., & Couch W. J. 2003, MNRAS, 344, 307
Márquez I., Masegosa J., Moles M., Varela J. Bettoni D., Galletta G. 2002, A&A, 393 389
Michel-Dansac L., Lambas D. G., Alonso M. S., & Tissera P. 2008, MNRAS, 386, L82
Mouhcine M., Baldry I. K., & Bamford S. P. 2007, MNRAS, 382, 801
Peeples M. S., Pogge R. W., & Stanek K. Z. 2009, ApJ, 695, 259
Pettini M., & Pagel B. E. J. 2004, MNRAS, 348, L59
Rupke D. S. N., Veilleux S., & Baker A. J. 2008, ApJ, 674, 172
Tremonti C. A. et al. 2004, ApJ, 613, 898
Zaritsky D., Kennicutt R. C., Jr., & Huchra J. P. 1994, ApJ, 420, 87